Appl Phys B (2011) 104:1001–1006
DOI 10.1007/s00340-011-4588-y

Applied Physics B
Lasers and Optics

Scintillation behavior of Laguerre Gaussian beams in strong turbulence

H.T. Eyyuboğlu · Y. Baykal · A. Falits

Received: 25 November 2010 / Revised version: 10 March 2011 / Published online: 3 June 2011

Abstract In strong atmospheric turbulence, the asymptotic on-axis scintillation behaviors of Laguerre Gaussian (LG) beams are examined. To arrive at the strong-turbulence solution, we utilize the existing filtering approach for weak-turbulence solutions and our recently reported weak-turbulence scintillation index formula for LG beams. In the limiting case, our solution correctly predicts the asymptotic strong-turbulence behavior of Gaussian beam wave scintillation. Investigation of the scintillations versus the propagation distance, source size, wavelength and refractive index structure parameter lead to the conclusion that the LG beams with higher order radial modes can provide less scintillation. The results are applicable to long-haul atmospheric optical communication links.

1 Introduction

The scintillation indices are found for different types of incidences [1–6], also for LG beams [7] in weak turbulence. These results are well accepted for horizontal atmospheric optical links having spans of only several kilometers. In telecommunication networks, these applications are known as access networks through which the high speed telecommunication core network is connected to the end users. Considering the core network, atmospheric optical links can be candidates to function as a high rate transport medium like optical fiber links of several tens of kilometers. In such a link span, one should consider scintillation solutions that are valid in strong turbulence.

Strong-turbulence effects have been studied for a long time [1, 8–18]. The first experimental evidence [8] and the first theoretical findings [9–12] of scintillations in strong atmospheric turbulence are reported long ago. The first evidence of applicability of phase approximation for describing the strong scintillation regime is provided in [13]. In the last decade, several investigations in strong turbulence are reported. Numerical simulation is applied to understand the irradiance variance variations [19] in strong atmospheric turbulence. Monostatic lidar [20], aperture averaging effects [21, 22] and communication system performance [23] in strong turbulence are reported. Recently, some literature has appeared, reporting the scintillation reductions obtained from the use of new beam types such as Airy beams [24], combined Gaussian vortex beams [25] and the use of multi-wavelength sources over extremely long (149 km) propagation distances [26]. To arrive at some of these results, simple tests are conducted using the computer modeled versions of atmospheric turbulence. Providing a complimentary approach to experiments, these models constitute a convenient way of verification for theoretical derivations. We hope to use such methods in our next series of studies.

In the current paper, we have formulated and evaluated the on-axis scintillation index of LG beams in strong turbulence by employing the extension of weak-turbulence scintillations through appropriate filtering [1]. Our motivation is

H.T. Eyyuboğlu (✉) · Y. Baykal
Department of Electronic and Communication Engineering,
Çankaya University, Öğretmenler Cad. No. 14 Yüzüncüyıl,
06530 Balgat, Ankara, Turkey
e-mail: h.eyyuboglu@cankaya.edu.tr
Fax: +90-312-2848043

Y. Baykal
e-mail: y.baykal@cankaya.edu.tr
Fax: +90-312-2848043

A. Falits
Zuev Institute of Atmospheric Optics, Tomsk, Russia
e-mail: falits@iao.ru
Fax: +7-3822-492086

to understand whether the use of LG beams in long-haul atmospheric optical links will bring any advantage in terms of intensity fluctuations. As explained in Sect. 2, the asymptotic strong-turbulence treatment is basically derived from that of weak-turbulence formulation. The adoption of this basic formulation to the case of LG beams in strong turbulence and the incorporation of the appropriate filtering arrangement are the essential new elements of this study.

2 Strong-turbulence treatment for LG beam

Examining the structures in (46) of Chap. 4, (14) of Chap. 8 and in (13), (14), (20) of Chap. 9 in [1] and the composition of the formulations in our previous studies [2–6], it is possible to deduce that the asymptotic on-axis scintillation index under strong-turbulence conditions is related to the one in weak turbulence in the following manner

$$m_{\mathrm{st}}^2 = 1 + 4m_{\mathrm{wt}}^2 \times \left(\kappa, \theta_\kappa, \eta, \exp\left\{-\int_0^1 D_S\left[\frac{z\kappa}{k} X(\tau,\eta)\right] d\tau\right\}\right), \quad (1)$$

where m_{st}^2 and $m_{\mathrm{wt}}^2(\ )$ respectively stand for the scintillation index formulation of strong and weak turbulence with $m_{\mathrm{wt}}^2(\ )$ still in integral form, hence κ and θ_κ are the spatial frequency variables, η is the distance variable, $D_S[\ ]$ is the phase structure function of plane wave containing in its argument the distance between transmitter and receiver $z, \kappa, k = 2\pi/\lambda$ with λ representing the wavelength of the source and a low pass filter function $X(\tau,\eta)$ associated with the radius of curvature of the beam in question. In this study, we shall adopt LG beam, which is defined on the source plane as

$$E_i(r_i,\theta_i) = \exp\left(-\frac{r_i^2}{\alpha_i^2}\right) L_p\left(2\frac{r_i^2}{\alpha_i^2}\right) \quad (2)$$

In (2), $E_i(r_i,\theta_i)$ is the optical field with radial and angular coordinates of r_i and θ_i, α_i is the Gaussian source size, p is the radial mode number for the Laguerre polynomial $L_p(\ )$.

For the LG beam described by (2), the formulation of m_{wt}^2 via Rytov method is provided in [7]. Therefore, to determine m_{st}^2, we need to specify the function $X(\tau,\eta)$ present in (1).

To do that, the radius of curvature expression of an LG beam propagating in free space is required [1]. Here we simplify matters and equate the radius of curvature of the beam in (2) to that of a collimated fundamental Gaussian beam. Thus, the radius of curvature $F(z)$ at an axial transmission point of z will be given by

$$F(z) = -\frac{k^2\alpha_i^4 + 4z^2}{4z}. \quad (3)$$

Subsequently, by employing (14) of Chap. 9 of [1], $X(\tau,\eta)$ will appear as

$$X(\tau,\eta) = \begin{cases} \tau[1+\frac{\eta}{F(z)}] \\ \frac{\eta}{z}[1+\frac{\tau z}{F(z)}] \end{cases} = \begin{cases} \tau(1-\frac{4z\eta}{k^2\alpha_i^4+4z^2}) & \text{if } \tau < \frac{\eta}{z}, \\ \frac{\eta}{z}(1-\frac{4z^2\tau}{k^2\alpha_i^4+4z^2}) & \text{if } \tau > \frac{\eta}{z}. \end{cases} \quad (4)$$

By inserting (4) into (1) and performing the integration by taking the phase structure function incorporating Kolmogorov spectrum, we get

$$\begin{aligned} &D_{S\kappa}(\kappa,\eta) \\ &= \int_0^1 D_S\left[\frac{z\kappa}{k} X(\tau,\eta)\right] d\tau \\ &= 0.3638 C_n^2 k^{1/3} z(\kappa\eta)^{5/3} \left\{3\left(\frac{\eta}{z}\right)\left(1-\frac{4z\eta}{k^2\alpha_i^4+4z^2}\right)^{5/3}\right. \\ &\quad + 0.75\frac{k^2\alpha_i^4+4z^2}{z^2}\left[\left(1-\frac{4z\eta}{k^2\alpha_i^4+4z^2}\right)^{8/3}\right. \\ &\quad \left.\left. - \left(1-\frac{4z^2}{k^2\alpha_i^4+4z^2}\right)^{8/3}\right]\right\}. \end{aligned} \quad (5)$$

Finally, combining (6) of [7] with (1) and (5) of this study and rearranging will deliver m_{st}^2 as

$$\begin{aligned} m_{\mathrm{st}}^2 = 1 &+ 10.4225 C_n^2 k^2 2^{2p} \int_0^z d\eta \int_0^\infty d\kappa\, \kappa^{-8/3} \\ &\times \exp\left[-D_{S\kappa}(\kappa,\eta)\right] \\ &\times \left\{\left[\frac{0.25k^4\alpha_i^8 + 4\eta^2 z^2 + k^2\alpha_i^4(\eta^2+z^2)}{(k^2\alpha_i^4+4\eta^2)(k^2\alpha_i^4+4z^2)}\right]^p\right. \\ &\times \exp\left[-\frac{2\alpha_i^2\kappa^2(z-\eta)^2}{k^2\alpha_i^4+4z^2}\right] \\ &\times \left| L_p\left\{ j\alpha_i^2 \right.\right. \\ &\left.\left. \times \frac{\kappa^2(z-\eta)^2(k\alpha_i^2+2j\eta)}{(k\alpha_i^2+2jz)[k\alpha_i^2(z-\eta)+j(0.5k^2\alpha_i^4+2\eta z)]} \right\}\right|^2 \\ &+ (-1)^{1+p}\,\mathrm{Re}\left[\left(\frac{k\alpha_i^2-2j\eta}{k\alpha_i^2-2jz}\right)^{2p}\right. \\ &\times \left[\frac{k\alpha_i^2(z-\eta)+j(0.5k^2\alpha_i^4+2\eta z)}{k^2\alpha_i^4+4\eta^2}\right]^{2p} \\ &\left.\times \exp\left[-\frac{j\kappa^2(z-\eta)(k\alpha_i^2+2j\eta)}{k(k\alpha_i^2+2jz)}\right]\right. \end{aligned}$$

$$\times \left(L_p \left\{ j\alpha_i^2 \times \frac{\kappa^2 (z-\eta)^2 (k\alpha_i^2 + 2j\eta)}{(k\alpha_i^2 + 2jL)[k\alpha_i^2 (z-\eta) + j(0.5k^2\alpha_i^4 + 2\eta z)]} \right\}^2 \right] \Bigg\}. \tag{6}$$

In (5) and (6), C_n^2 denotes the refractive index structure parameter and $j = (-1)^{0.5}$. Equation (6) reduces to (20) in Sect. 9.3.2 of [1] at the Gaussian limit.

3 Graphical illustrations

We illustrate in this section, the variations of on scintillation index against propagation distance, source size, wavelength and the refractive index structure parameter at different radial mode numbers. This is done by numerically evaluating the double integral in (6) by using a modified version of a previously introduced integral routine [27]. To effectively use the capabilities of the double integral routine in question, it is important to realize that in (6) a big portion of the integrand over κ is concentrated in close proximity to zero. Therefore to allow a proper evaluation of the inner integral in (6), we have subdivided the total integration range from zero up to infinity into tiny steps around zero and rather large steps around infinity represented by the number 10 000.

It should be kept in mind that the formulation offered in (6) is valid for the scintillation behavior in an asymptotic form and under strong-turbulence conditions. To ensure that we are always in the strong-turbulence region, in the following graphs, the source and propagation parameters are chosen such that $1.23C_n^2 k^{7/6} z^{11/6} \gg 1$ is always satisfied. All throughout the graphs, a single set of radial mode numbers is used, that is, $p = 0, 1, 2, 5, 8$.

First we analyze in Fig. 1, the dependence of scintillations against propagation distance. From Fig. 1, we note that all beams act nearly in the same way, i.e. their scintillations will experience a fall with rising propagation distance, eventually merging toward the same saturation value. Bearing in mind that in Fig. 1, $p = 0$ refers to the fundamental Gaussian beam, we see that the behavior displayed in Fig. 1 is in conformity with the one exhibited in [1]; furthermore, the LG beams $p \geq 1$ have similar scintillation property, but their higher radial mode numbers will help reduce scintillations. It is seen from the illustrations in [7], greater p values of LG beams lead to the creation of side lobes nearer to the on-axis position. As the propagation of the beam advances, the intensity of these side lobes initially tend to concentrate around on-axis, thereby increasing the intensity levels at this position. Since scintillation index acts inversely proportional to intensity levels [28], rising p values would inevitably cause scintillation reductions. Note that these statements are valid for relatively shorter propagation distances, because as the propagation distance is increased indefinitely, all beams converge into a Gaussian profile [29], thus eliminating the initial differences. This effect is also clearly visible in Fig. 1. As already pointed out, the behavior seen in Fig. 1 is in conformity with [1], in particular with the graphical illustrations of Figs. 9.14 and 9.15 in Sect. 9.6 of [1] and similar curves of [20], where theoretical curves as well as experimental results are exhibited. We should of course bear in mind that our formulation covers the asymptotic treatment of the scintillation index in strong-turbulence region. Therefore it is not possible to observe in Fig. 1, the weak scintillation parts and the bending transitions from the weak region to strong region. To plot the scintillation index variation across the whole range of weak, moderate and strong-turbulence regions, a complete

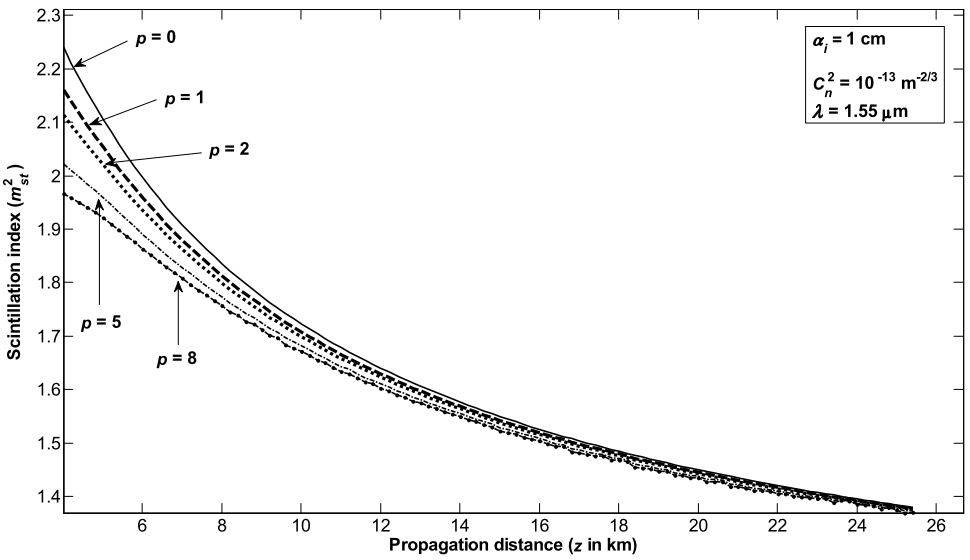

Fig. 1 Scintillation index variation versus propagation distance at different radial mode numbers and at $\alpha_i = 1$ cm, $C_n^2 = 10^{-13}$ m$^{-2/3}$, $\lambda = 1.55$ μm

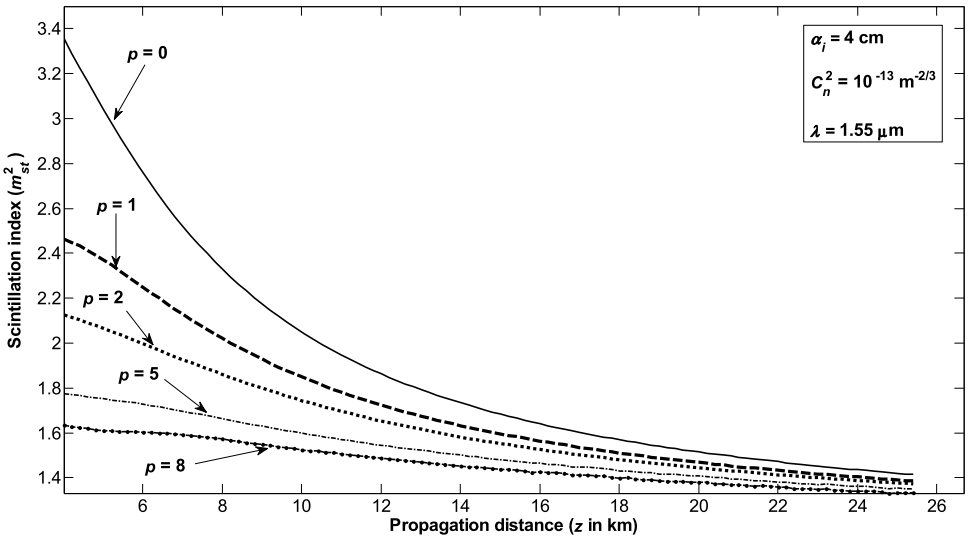

Fig. 2 Scintillation index variation versus propagation distance at different radial mode numbers and at $\alpha_i = 4$ cm, $C_n^2 = 10^{-13}$ m$^{-2/3}$, $\lambda = 1.55$ μm

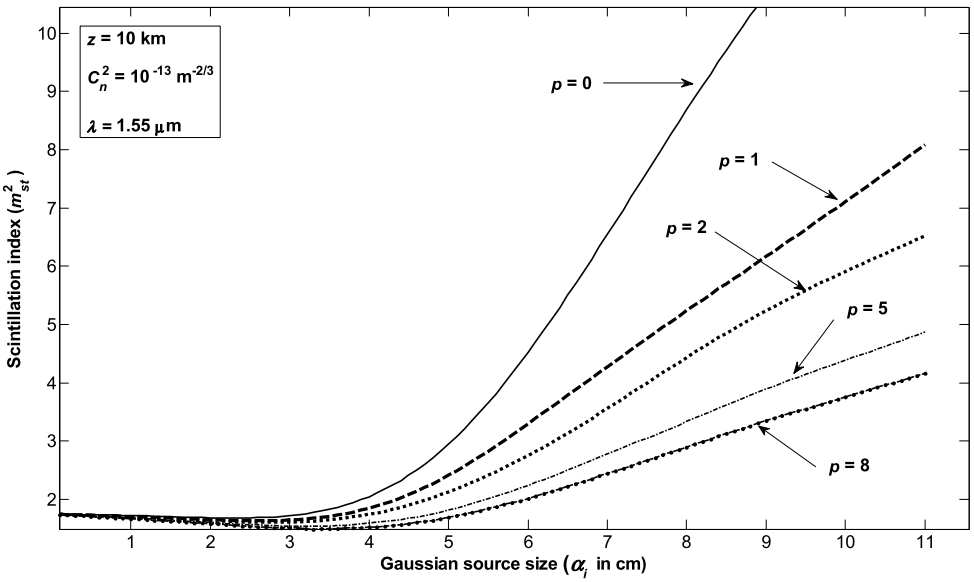

Fig. 3 Scintillation index variation versus source size at different radial mode numbers and $z = 10$ km, $C_n^2 = 10^{-13}$ m$^{-2/3}$, $\lambda = 1.55$ μm

different approach, i.e., a return to the very beginning of the scintillation formulation is required as detailed in [1, 18, 20, 30]. And this is not the intention in the present paper. In its present form, however, our formulation yields the correct scintillation values at the limiting case of $p = 0$ for strong-turbulence cases. To this end, a test was made by inserting the source and propagation parameters used in Figs. 9.14 and 9.15 in Sect. 9.6 of [1] into (6) and it was seen that (6) would produce identical results as displayed in Figs. 9.14–9.15 in Sect. 9.6 of [1] for strong-turbulence regimes.

Next, in Fig. 2, the case of a larger source size is examined for the beams of Fig. 1. Comparison of Fig. 1 and Fig. 2 shows that as the source size becomes larger, we will witness an increase in scintillations for LG beams with lower radial mode numbers, while the scintillations of beams of higher radial orders will drop. Joint examination of Figs. 1 and 2 further illustrates that the ordering of beams will not change with rising source size, that is, scintillations will still be the smallest for the LG beams of highest radial mode number.

The dependence of the scintillation index on the source size is explored in Fig. 3, where it is seen that there will be little amount of scintillations for source sizes up to approximately 4 cm, but from then onwards there will be high rises, in particular for beams with small radial mode numbers. It is also revealed by Fig. 3 that, within a range of small source sizes up to 4 cm, scintillations will slightly decrease, particularly at higher radial mode numbers. Such decreases are in conformity with the situation encountered in Fig. 2.

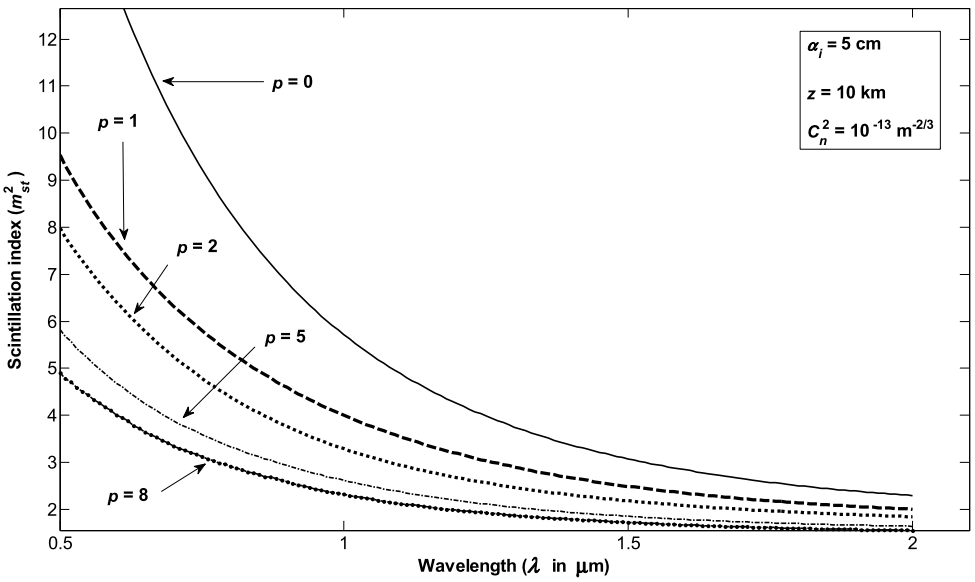

Fig. 4 Scintillation index variation versus wavelength at different radial mode numbers and $\alpha_i = 5$ cm, $z = 10$ km, $C_n^2 = 10^{-13}$ m$^{-2/3}$

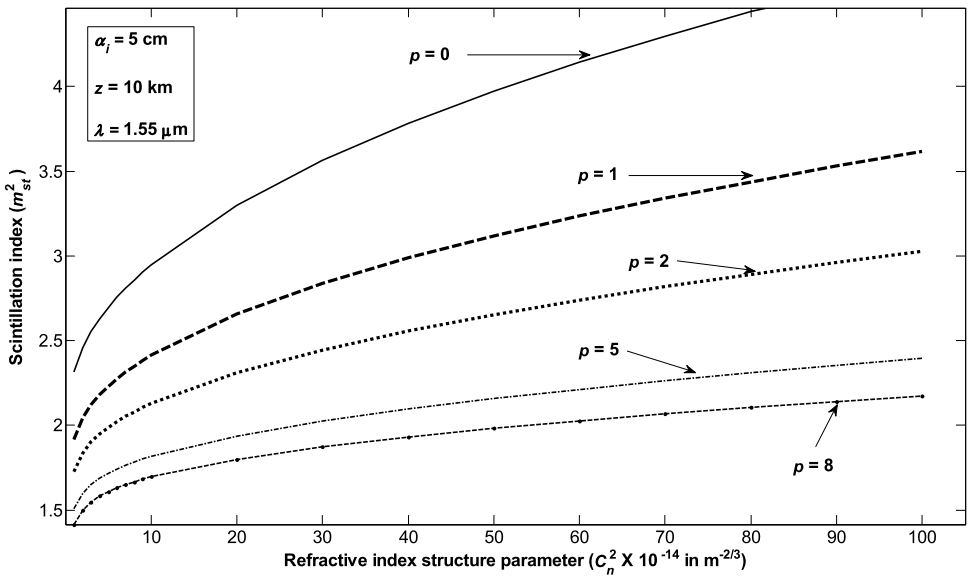

Fig. 5 Scintillation index variation versus refractive index structure parameter at different radial mode numbers and $\alpha_i = 5$ cm, $z = 10$ km, $\lambda = 1.55$ µm

Scintillation index variation with wavelength is investigated in Fig. 4. The trend of scintillations falling at longer wavelengths as found in Fig. 4 matches with the weak scintillation behaviors observed in [2, 4]. It is also noted from Fig. 4 that the case of LG beams with higher radial mode numbers offering least scintillations is applicable all throughout the wavelength range considered. Finally the variation against the refractive index structure parameter is examined in Fig. 5 which shows that scintillations will increase in a logarithmic manner with increases in C_n^2 values. It is important to point out that this kind of behavior is somewhat different from the one found for weak scintillations and it is possible to see from (5) and (6) that such a behavior in strong turbulence arises due to the presence of low pass filtering function.

4 Conclusion

The scintillation index of LG beams in strong turbulence is formulated and evaluated. Examining the scintillations versus the propagation distance shows that the higher radial modes will exhibit lower scintillations, but will merge to the same saturation value as the propagation distance is greatly extended. At larger source sizes the same situation holds with scintillations of lower radial order beams attaining rather large scintillation levels. Similar to the weak-turbulence case, scintillations of strong turbulence will also have a falling trend against rising wavelengths. Increasing values of the refractive index structure parameter will cause scintillations to increase in a logarithmic manner. In all the cases considered, it is found that LG beams of higher radial

order will uniformly create less scintillation under strong-turbulence conditions.

Acknowledgements This study was performed within the framework of the joint research project between The Scientific and Technological Research Council of Turkey (Tübitak) and The Russian Foundation for Basic Research (RFBR) entitled, "Effects of source beam types on optical wave propagation in turbulent atmosphere". The authors would like to express their gratitude to Tübitak and RFBR and the hosting institutions, Çankaya University and Zuev Institute of Atmospheric Optics (IAO SB RAS). We would also like to thank Dr. Emre Sermutlu for the original design and the revision of the double quadruple routine that was used in the numeric evaluation of (6).

References

1. L.C. Andrews, R.L. Phillips, *Laser Beam Propagation through Random Media* (SPIE, Bellingham, 2005)
2. Y. Baykal, H.T. Eyyuboğlu, Appl. Opt. **45**, 3793 (2006)
3. H.T. Eyyuboğlu, Y. Baykal, Appl. Opt. **46**, 1099 (2007)
4. Y. Cai, H.T. Eyyuboğlu, Y. Baykal, J. Opt. Soc. Am. A **25**, 1497 (2008)
5. H.T. Eyyuboğlu, Y. Baykal, E. Sermutlu, Y. Cai, Appl. Phys. B **92**, 229 (2008)
6. H.T. Eyyuboğlu, E. Sermutlu, Y. Baykal, Y. Cai, O. Korotkova, Appl. Phys. B **93**, 605 (2008)
7. H.T. Eyyuboğlu, Y. Baykal, X. Ji, Appl. Phys. B **98**, 857 (2010)
8. M.E. Gracheva, A.S. Gurvich, VUZ Izv. Radiofiz. **8**, 718 (1965)
9. K.S. Gochelashvily, V.I. Shishov, Opt. Acta **18**, 313 (1971)
10. K.S. Gochelashvily, V.I. Shishov, Opt. Acta **19**, 327 (1972)
11. K.S. Gochelashvily, Opt. Acta **20**, 193 (1973)
12. K.S. Gochelashvily, V.I. Shishov, Opt. Acta **18**, 767 (1971)
13. V.A. Banakh, G.M. Krekov, V.L. Mironov, S.S. Khmelevtsov, R.Sh. Tsvik, J. Opt. Soc. Am. **64**, 516 (1974)
14. R.S. Lawrence, J.W. Strohbehn, J. Opt. Soc. Am. **58**, 1523 (1970)
15. K.S. Gochelashvili, V.I. Shishov, Sov. Phys. JETP **39**, 605 (1974)
16. R.L. Phillips, L.C. Andrews, J. Opt. Soc. Am. **72**, 864 (1982)
17. S.M. Flatte, G.Y. Wang, J. Martin, J. Opt. Soc. Am. A **10**, 2363 (1993)
18. L.C. Andrews, R.L. Phillips, C.Y. Hopen, M.A. Al-Habash, J. Opt. Soc. Am. A **16**, 1417 (1999)
19. S.M. Flatte, J.S. Gerber, J. Opt. Soc. Am. A **17**, 1092 (2000)
20. L.C. Andrews, R.L. Phillips, Waves Random Media **11**, 233 (2001)
21. F.S. Vetelino, C. Young, L. Andrews, J. Recolons, Appl. Opt. **46**, 2099 (2007)
22. F.S. Vetelino, C. Young, L. Andrews, Appl. Opt. **46**, 3780 (2007)
23. I.B. Djordjevic, G.T. Djordjevic, Opt. Express **17**, 18250 (2009)
24. G. Gbur, Y. Gu, Proc. SPIE **7924-02**, 202 (2011)
25. G.P. Berman, Proc. SPIE **7924-15**, 202 (2011)
26. M.A. Vorontsov, Proc. SPIE **7924-07**, 202 (2011)
27. H.T. Eyyuboğlu, Appl. Phys. B **88**, 259 (2007)
28. H.T. Eyyuboğlu, Appl. Phys. B **88**, 301 (2009)
29. H.T. Eyyuboğlu, Y. Baykal, E. Sermutlu, Opt. Commun. **265**, 399 (2006)
30. H. Gerçekçioğlu, Y. Baykal, C. Nakiboğlu, J. Opt. Soc. Am. A **27**, 1834 (2010)